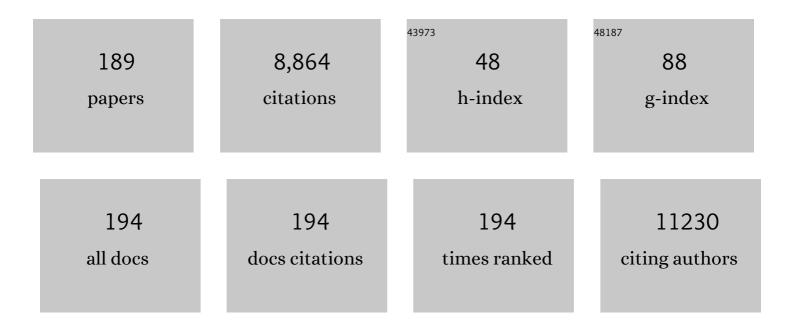
List of Publications by Year in descending order

Source: https://exaly.com/author-pdf/146048/publications.pdf Version: 2024-02-01



SHUN WANC

#	Article	IF	CITATIONS
1	Revisiting the Role of Polysulfides in Lithium–Sulfur Batteries. Advanced Materials, 2018, 30, e1705590.	11.1	456
2	A Singleâ€Atom Iridium Heterogeneous Catalyst in Oxygen Reduction Reaction. Angewandte Chemie - International Edition, 2019, 58, 9640-9645.	7.2	312
3	The Cathode Choice for Commercialization of Sodiumâ€ion Batteries: Layered Transition Metal Oxides versus Prussian Blue Analogs. Advanced Functional Materials, 2020, 30, 1909530.	7.8	276
4	Graphene Quantum Dots Supported by Graphene Nanoribbons with Ultrahigh Electrocatalytic Performance for Oxygen Reduction. Journal of the American Chemical Society, 2015, 137, 7588-7591.	6.6	262
5	Polymerâ€Templated Formation of Polydopamineâ€Coated SnO <sub>2</sub> Nanocrystals: Anodes for Cyclable Lithiumâ€Ion Batteries. Angewandte Chemie - International Edition, 2017, 56, 1869-1872.	7.2	260
6	Recent Progress of Layered Transition Metal Oxide Cathodes for Sodiumâ€ion Batteries. Small, 2019, 15, e1805381.	5.2	246
7	Sodium transition metal oxides: the preferred cathode choice for future sodium-ion batteries?. Energy and Environmental Science, 2021, 14, 158-179.	15.6	224
8	Recent Progress in Biomassâ€Đerived Electrode Materials for High Volumetric Performance Supercapacitors. Advanced Energy Materials, 2018, 8, 1801007.	10.2	213
9	Chemisorption of polysulfides through redox reactions with organic molecules for lithium–sulfur batteries. Nature Communications, 2018, 9, 705.	5.8	207
10	High Volumetric Capacitance, Ultralong Life Supercapacitors Enabled by Waxberryâ€Derived Hierarchical Porous Carbon Materials. Advanced Energy Materials, 2018, 8, 1702695.	10.2	204
11	Extraordinarily High Activity in the Hydrodesulfurization of 4,6-Dimethyldibenzothiophene over Pd Supported on Mesoporous Zeolite Y. Journal of the American Chemical Society, 2011, 133, 15346-15349.	6.6	186
12	Heteroatomâ€Đoped Porous Carbon Materials with Unprecedented High Volumetric Capacitive Performance. Angewandte Chemie - International Edition, 2019, 58, 2397-2401.	7.2	178
13	Thermodynamic Analysis of Decomposition of Thiourea and Thiourea Oxides. Journal of Physical Chemistry B, 2005, 109, 17281-17289.	1.2	169
14	Scrutinizing Defects and Defect Density of Seleniumâ€Doped Graphene for Highâ€Efficiency Triiodide Reduction in Dyeâ€Sensitized Solar Cells. Angewandte Chemie - International Edition, 2018, 57, 4682-4686.	7.2	155
15	Molybdenum Carbide Nanoparticles Coated into the Graphene Wrapping Nâ€Đoped Porous Carbon Microspheres for Highly Efficient Electrocatalytic Hydrogen Evolution Both in Acidic and Alkaline Media. Advanced Science, 2018, 5, 1700733.	5.6	152
16	Facile Synthesis of Hierarchical Hollow CoP@C Composites with Superior Performance for Sodium and Potassium Storage. Angewandte Chemie - International Edition, 2020, 59, 5159-5164.	7.2	142
17	The charge carrier dynamics, efficiency and stability of two-dimensional material-based perovskite solar cells. Chemical Society Reviews, 2019, 48, 4854-4891.	18.7	139
18	Hybrid Organic–Inorganic Thermoelectric Materials and Devices. Angewandte Chemie - International Edition, 2019, 58, 15206-15226.	7.2	138

#	Article	IF	CITATIONS
19	Sulfurâ€Impregnated, Sandwichâ€Type, Hybrid Carbon Nanosheets with Hierarchical Porous Structure for Highâ€Performance Lithiumâ€Sulfur Batteries. Advanced Energy Materials, 2014, 4, 1301988.	10.2	130
20	Structural design of anode materials for sodium-ion batteries. Journal of Materials Chemistry A, 2018, 6, 6183-6205.	5.2	127
21	The Preparation of Hierarchical Flowerlike NiO/Reduced Graphene Oxide Composites for High Performance Supercapacitor Applications. Energy & Fuels, 2013, 27, 6304-6310.	2.5	111
22	Aqueous intercalation-type electrode materials for grid-level energy storage: Beyond the limits of lithium and sodium. Nano Energy, 2018, 50, 229-244.	8.2	108
23	Hierarchically Porous Multimetalâ€Based Carbon Nanorod Hybrid as an Efficient Oxygen Catalyst for Rechargeable Zinc–Air Batteries. Advanced Functional Materials, 2020, 30, 1908167.	7.8	105
24	Synergistic Cascade Carrier Extraction via Dual Interfacial Positioning of Ambipolar Black Phosphorene for Highâ€Efficiency Perovskite Solar Cells. Advanced Materials, 2020, 32, e2000999.	11.1	104
25	P2-type Na <sub>2/3</sub> Ni <sub>1/3</sub> Mn <sub>2/3</sub> O <sub>2</sub> as a cathode material with high-rate and long-life for sodium ion storage. Journal of Materials Chemistry A, 2019, 7, 9215-9221.	5.2	102
26	Origins of Boosted Charge Storage on Heteroatomâ€Đoped Carbons. Angewandte Chemie - International Edition, 2020, 59, 7928-7933.	7.2	102
27	A Novel Graphene Oxide Wrapped Na <sub>2</sub> Fe <sub>2</sub> (SO <sub>4</sub> ) <sub>3</sub> /C Cathode Composite for Long Life and High Energy Density Sodiumâ€lon Batteries. Advanced Energy Materials, 2018, 8, 1800944.	10.2	101
28	Ultrathin 2D TiS <sub>2</sub> Nanosheets for High Capacity and Longâ€Life Sodium Ion Batteries. Advanced Energy Materials, 2019, 9, 1803210.	10.2	100
29	Radially Inwardly Aligned Hierarchical Porous Carbon for Ultraâ€Longâ€Life Lithium–Sulfur Batteries. Angewandte Chemie - International Edition, 2020, 59, 6406-6411.	7.2	100
30	A Versatile Strategy for Shish-Kebab-like Multi-heterostructured Chalcogenides and Enhanced Photocatalytic Hydrogen Evolution. Journal of the American Chemical Society, 2015, 137, 11004-11010.	6.6	95
31	A Robust Route to Co <sub>2</sub> (OH) <sub>2</sub> CO <sub>3</sub> Ultrathin Nanosheets with Superior Lithium Storage Capability Templated by Aspartic Acidâ€Functionalized Graphene Oxide. Advanced Energy Materials, 2019, 9, 1901093.	10.2	94
32	An electrochemical impedance sensor for the label-free ultrasensitive detection of interleukin-6 antigen. Sensors and Actuators B: Chemical, 2013, 178, 310-315.	4.0	88
33	Electrochemical detection of hepatitis B and papilloma virus DNAs using SWCNT array coated with gold nanoparticles. Biosensors and Bioelectronics, 2013, 41, 205-210.	5.3	88
34	3D hierarchical nitrogen-doped carbon nanoflower derived from chitosan for efficient electrocatalytic oxygen reduction and high performance lithium–sulfur batteries. Journal of Materials Chemistry A, 2017, 5, 18193-18206.	5.2	86
35	In Situ Encapsulation of Iron Complex Nanoparticles into Biomassâ€Derived Heteroatomâ€Enriched Carbon Nanotubes for Highâ€Performance Supercapacitors. Advanced Energy Materials, 2019, 9, 1803221.	10.2	86
36	Nitrogen and sulfur co-doped porous carbon sheets for energy storage and pH-universal oxygen reduction reaction. Nano Energy, 2018, 54, 192-199.	8.2	83

#	Article	IF	CITATIONS
37	Direct Observation of Defectâ€Aided Structural Evolution in a Nickelâ€Rich Layered Cathode. Angewandte Chemie - International Edition, 2020, 59, 22092-22099.	7.2	75
38	A Triphasic Bifunctional Oxygen Electrocatalyst with Tunable and Synergetic Interfacial Structure for Rechargeable Znâ€Air Batteries. Advanced Energy Materials, 2020, 10, 1903003.	10.2	74
39	Fundamentals of Electrolytes for Solid-State Batteries: Challenges and Perspectives. Frontiers in Materials, 2020, 7, .	1.2	72
40	SnO <sub>2</sub> as Advanced Anode of Alkaliâ€ion Batteries: Inhibiting Sn Coarsening by Crafting Robust Physical Barriers, Void Boundaries, and Heterophase Interfaces for Superior Electrochemical Reaction Reversibility. Advanced Energy Materials, 2020, 10, 1902657.	10.2	71
41	Synthesis of Au-Decorated Tripod-Shaped Te Hybrids for Applications in the Ultrasensitive Detection of Arsenic. ACS Applied Materials & Interfaces, 2013, 5, 5733-5740.	4.0	68
42	Novel Nonâ€Carbon Sulfur Hosts Based on Strong Chemisorption for Lithium–Sulfur Batteries. Small, 2018, 14, e1801987.	5.2	68
43	Halide Perovskite Materials for Photo(Electro)Chemical Applications: Dimensionality, Heterojunction, and Performance. Advanced Energy Materials, 2022, 12, 2004002.	10.2	68
44	Reconfigurable Plasmonic Diastereomers Assembled by DNA Origami. ACS Nano, 2019, 13, 13702-13708.	7.3	66
45	Incorporating ultra-small N-doped Mo2C nanoparticles onto 3D N-doped flower-like carbon nanospheres for robust electrocatalytic hydrogen evolution. Nano Energy, 2021, 86, 106047.	8.2	66
46	A Singleâ€Atom Iridium Heterogeneous Catalyst in Oxygen Reduction Reaction. Angewandte Chemie, 2019, 131, 9742-9747.	1.6	59
47	Graphene Oxide Liquid Crystals as a Versatile and Tunable Alignment Medium for the Measurement of Residual Dipolar Couplings in Organic Solvents. Journal of the American Chemical Society, 2014, 136, 11280-11283.	6.6	58
48	Insights of Heteroatoms Dopingâ€Enhanced Bifunctionalities on Carbon Based Energy Storage and Conversion. Advanced Functional Materials, 2021, 31, 2009109.	7.8	58
49	Research Development on Aqueous Ammoniumâ€Ion Batteries. Advanced Functional Materials, 2022, 32, .	7.8	58
50	Controllable synthesis of highly uniform flower-like hierarchical carbon nanospheres and their application in high performance lithium–sulfur batteries. Journal of Materials Chemistry A, 2017, 5, 6245-6256.	5.2	48
51	A Novel Glucose/pH Responsive Low-Molecular-Weight Organogel of Easy Recycling. Langmuir, 2013, 29, 13568-13575.	1.6	47
52	Single-crystal NaY(MoO4)2 thin plates with dominant {001} facets for efficient photocatalytic degradation of dyes under visible light irradiation. Chemical Communications, 2011, 47, 8013.	2.2	46
53	Aligned SWCNT-copper oxide array as a nonenzymatic electrochemical probe of glucose. Electrochemistry Communications, 2011, 13, 363-365.	2.3	45
54	Reaction inhomogeneity coupling with metal rearrangement triggers electrochemical degradation in lithium-rich layered cathode. Nature Communications, 2021, 12, 5370.	5.8	44

#	Article	IF	CITATIONS
55	Ultrasensitive room-temperature detection of NO2 with tellurium nanotube based chemiresistive sensor. Sensors and Actuators B: Chemical, 2014, 196, 321-327.	4.0	43
56	Tailoring Hierarchically Porous Nitrogenâ€, Sulfurâ€Codoped Carbon for Highâ€Performance Supercapacitors and Oxygen Reduction. Small, 2020, 16, e1906584.	5.2	43
57	Hydroxylated Multiâ€Walled Carbon Nanotubes Covalently Modified with Tris(hydroxypropyl) Phosphine as a Functional Interlayer for Advanced Lithium–Sulfur Batteries. Angewandte Chemie - International Edition, 2022, 61, .	7.2	43
58	Facile Preparation of Superhydrophobic Biomimetic Surface Based on Octadecyltrichlorosilane and Silica Nanoparticles. ACS Applied Materials & Interfaces, 2010, 2, 2393-2398.	4.0	42
59	Mildâ€Temperature Solutionâ€Assisted Encapsulation of Phosphorus into ZIFâ€8 Derived Porous Carbon as Lithiumâ€Ion Battery Anode. Small, 2020, 16, e1907141.	5.2	42
60	Synthesis, characterization and optical properties of flower-like tellurium. CrystEngComm, 2010, 12, 166-171.	1.3	40
61	Rapid and Controllable Synthesis of Nanocrystallized Nickelâ€Cobalt Boride Electrode Materials via a Mircoimpinging Stream Reaction for High Performance Supercapacitors. Small, 2020, 16, e2003342.	5.2	39
62	Single Mo–N <sub>4</sub> Atomic Sites Anchored on Nâ€doped Carbon Nanoflowers as Sulfur Host with Multiple Immobilization and Catalytic Effects for Highâ€Performance Lithium–Sulfur Batteries. Advanced Functional Materials, 2022, 32, .	7.8	39
63	Study of hydrodesulfurization of 4,6-DM-DBT over Pd supported on mesoporous USY zeolite. Applied Catalysis A: General, 2012, 433-434, 251-257.	2.2	38
64	Deep-Breathing Honeycomb-like Co-Nx-C Nanopolyhedron Bifunctional Oxygen Electrocatalysts for Rechargeable Zn-Air Batteries. IScience, 2020, 23, 101404.	1.9	38
65	Recent advances in solarâ€driven CO <sub>2</sub> reduction over gâ€C <sub>3</sub> N <sub>4</sub> â€based photocatalysts. , 2023, 5, .		38
66	Zero discharge process for foil industry waste acid reclamation: Coupling of diffusion dialysis and electrodialysis with bipolar membranes. Journal of Membrane Science, 2013, 432, 90-96.	4.1	37
67	Challenges of layer-structured cathodes for sodium-ion batteries. Nanoscale Horizons, 2022, 7, 338-351.	4.1	37
68	Synthesis of Porous NiO/Reduced Graphene Oxide Composites for Supercapacitors. Journal of the Electrochemical Society, 2012, 159, A990-A994.	1.3	36
69	Integrated dynamic wet spinning of core-sheath hydrogel fibers for optical-to-brain/tissue communications. National Science Review, 2021, 8, nwaa209.	4.6	36
70	Identification of the Structures of Superlong Oriented Single-Walled Carbon Nanotube Arrays by Electrodeposition of Metal and Raman Spectroscopy. Journal of the American Chemical Society, 2008, 130, 11860-11861.	6.6	35
71	Interfacial Strategies for Suppression of Mn Dissolution in Rechargeable Battery Cathode Materials. ACS Applied Materials & Interfaces, 2022, 14, 23022-23032.	4.0	35
72	Heteroatomâ€Doped Porous Carbon Materials with Unprecedented High Volumetric Capacitive Performance. Angewandte Chemie, 2019, 131, 2419-2423.	1.6	34

#	Article	IF	CITATIONS
73	The Emerging Electrochemical Activation Tactic for Aqueous Energy Storage: Fundamentals, Applications, and Future. Advanced Functional Materials, 2022, 32, .	7.8	34
74	Advancing Performance and Unfolding Mechanism of Lithium and Sodium Storage in SnO <sub>2</sub> via Precision Synthesis of Monodisperse PEG‣igated Nanoparticles. Advanced Energy Materials, 2022, 12, .	10.2	34
75	Electrochemical growth of gold nanoparticles on horizontally aligned carbon nanotubes: A new platform for ultrasensitive DNA sensing. Biosensors and Bioelectronics, 2012, 33, 279-283.	5.3	33
76	Photothermal effect enables markedly enhanced oxygen reduction and evolution activities for high-performance Zn–air batteries. Journal of Materials Chemistry A, 2021, 9, 19734-19740.	5.2	33
77	Urchin-Shaped Bi <sub>2</sub> S <sub>3</sub> /Cu <sub>2</sub> S/Cu <sub>3</sub> BiS <sub>3</sub> Composites with Enhanced Photothermal and CT Imaging Performance. Journal of Physical Chemistry C, 2018, 122, 3794-3800.	1.5	32
78	Encapsulating phosphorus inside carbon nanotubes via a solution approach for advanced lithium ion host. Nano Energy, 2019, 58, 23-29.	8.2	32
79	Cascade signal amplification for electrochemical immunosensing by integrating biobarcode probes, surface-initiated enzymatic polymerization and silver nanoparticle deposition. Biosensors and Bioelectronics, 2015, 66, 177-183.	5.3	31
80	Highly sensitive and selective electrochemical detection of Hg2+ through surface-initiated enzymatic polymerization. Biosensors and Bioelectronics, 2016, 80, 105-110.	5.3	30
81	Tailoring conductive networks within hollow carbon nanospheres to host phosphorus for advanced sodium ion batteries. Nano Energy, 2020, 70, 104569.	8.2	29
82	Facile Synthesis of Birnessite δ-MnO <sub>2</sub> and Carbon Nanotube Composites as Effective Catalysts for Li-CO <sub>2</sub> Batteries. ACS Applied Materials & Interfaces, 2021, 13, 16585-16593.	4.0	29
83	Scrutinizing Defects and Defect Density of Seleniumâ€Doped Graphene for Highâ€Efficiency Triiodide Reduction in Dyeâ€Sensitized Solar Cells. Angewandte Chemie, 2018, 130, 4772-4776.	1.6	28
84	One-step nonlinear electrochemical synthesis of TexSy@PANI nanorod materials for Li-TexSy battery. Energy Storage Materials, 2019, 16, 31-36.	9.5	28
85	Fast coprecipitation of nickel-cobalt oxide in a micro-impinging stream reactor for the construction of high-performance asymmetric supercapacitors. Journal of Alloys and Compounds, 2019, 792, 314-327.	2.8	27
86	Hydrogen evolution reaction catalyzed by nickel/nickel phosphide nanospheres synthesized through electrochemical methods. Electrochimica Acta, 2019, 298, 229-236.	2.6	27
87	Polymerâ€Templated Formation of Polydopamineâ€Coated SnO <sub>2</sub> Nanocrystals: Anodes for Cyclable Lithiumâ€Ion Batteries. Angewandte Chemie, 2017, 129, 1895-1898.	1.6	26
88	Two 2-D homometallic and heterometallic Schiff-base complexes bridged by dicyanamide. Inorganic Chemistry Communication, 2009, 12, 255-258.	1.8	23
89	Strong Graphene 3D Assemblies with High Elastic Recovery and Hardness. Advanced Materials, 2018, 30, e1707424.	11.1	22
90	Scalable fabrication of geometry-tunable self-aligned superlattice photonic crystals for spectrum-programmable light trapping. Nano Energy, 2019, 58, 543-551.	8.2	22

#	Article	IF	CITATIONS
91	Enhanced Potassium Storage Capability of Two-Dimensional Transition-Metal Chalcogenides Enabled by a Collective Strategy. ACS Applied Materials & Interfaces, 2021, 13, 18838-18848.	4.0	21
92	Origins of Boosted Charge Storage on Heteroatomâ€Doped Carbons. Angewandte Chemie, 2020, 132, 8002-8007.	1.6	20
93	Cationic–anionic redox couple gradient to immunize against irreversible processes of Li-rich layered oxides. Journal of Materials Chemistry A, 2021, 9, 2325-2333.	5.2	20
94	Facile Synthesis of Hierarchical Hollow CoP@C Composites with Superior Performance for Sodium and Potassium Storage. Angewandte Chemie, 2020, 132, 5197-5202.	1.6	19
95	Understanding the Ni-rich layered structure materials for high-energy density lithium-ion batteries. Materials Chemistry Frontiers, 2021, 5, 2607-2622.	3.2	19
96	Structural engineering of electrode materials to boost high-performance sodium-ion batteries. Cell Reports Physical Science, 2021, 2, 100551.	2.8	19
97	Photo-Thermo-Mechanochemical Approach to Synthesize Quinolines via Addition/Cyclization of Sulfoxonium Ylides with 2-Vinylanilines Catalyzed by Iron(II) Phthalocyanine. Organic Letters, 2022, 24, 1146-1151.	2.4	19
98	Large-scale synthesis of feather-like single-crystal Te via a biphasic interfacial reaction route. CrystEngComm, 2010, 12, 3852.	1.3	18
99	Urchin-shaped MoS2–Cd0.8Zn0.2S nanocomposites with greatly enhanced and long-lasting photocatalytic activity. International Journal of Hydrogen Energy, 2017, 42, 18824-18831.	3.8	18
100	Tuning the NIR photoabsorption of CuWO <sub>4â^'x</sub> nanodots with oxygen vacancies for CT imaging guided photothermal therapy of tumors. Biomaterials Science, 2019, 7, 4651-4660.	2.6	18
101	Toward High-Performance Lithium–Sulfur Batteries: Efficient Anchoring and Catalytic Conversion of Polysulfides Using P-Doped Carbon Foam. ACS Applied Materials & Interfaces, 2021, 13, 50093-50100.	4.0	18
102	Determination of amino acids in by high performance capillary electrophoresis. Talanta, 2005, 66, 755-761.	2.9	17
103	Nano-TiO <sub>2</sub> : An Efficient and Reusable Heterogeneous Catalyst for Ring Opening of Epoxides Under Solvent-Free Conditions. Synthetic Communications, 2012, 42, 2440-2452.	1.1	17
104	A highly efficient reusable homogeneous copper catalyst for the selective aerobic oxygenation sulfides to sulfoxides. Tetrahedron Letters, 2018, 59, 982-986.	0.7	17
105	Surface lattice engineering for fine-tuned spatial configuration of nanocrystals. Nature Communications, 2021, 12, 5661.	5.8	17
106	Structure engineering of PtCu3/C catalyst from disordered to ordered intermetallic compound with heat-treatment for the methanol electrooxidation reaction. Nano Research, 2022, 15, 3866-3871.	5.8	17
107	Development of novel highly stable synergistic quaternary photocatalyst for the efficient hydrogen evolution reaction. Applied Surface Science, 2020, 510, 145498.	3.1	16
108	The enhanced electrocatalytic activity of graphene co-doped with chlorine and fluorine atoms. Electrochimica Acta, 2015, 177, 36-42.	2.6	15

#	Article	IF	CITATIONS
109	Radially Inwardly Aligned Hierarchical Porous Carbon for Ultra‣ong‣ife Lithium–Sulfur Batteries. Angewandte Chemie, 2020, 132, 6468-6473.	1.6	15
110	Self-assembly of osmium complexes on reduced graphene oxide: A case study toward electrochemical chiral sensing. Electrochemistry Communications, 2012, 16, 80-83.	2.3	14
111	Iron and Nitrogen Coâ€Doped Mesoporous Carbonâ€Based Heterogeneous Catalysts for Selective Reduction of Nitroarenes. Advanced Synthesis and Catalysis, 2019, 361, 3525-3531.	2.1	14
112	Unprecedently low thermal conductivity of unique tellurium nanoribbons. Nano Research, 2021, 14, 4725-4731.	5.8	14
113	Novel engineering of rutheniumâ€based electrocatalysts for acidic water oxidation: A mini review. Engineering Reports, 2021, 3, e12437.	0.9	14
114	Dual cocatalyst modified CdS achieving enhanced photocatalytic H2 generation and benzylamine oxidation performance. Applied Surface Science, 2022, 592, 153277.	3.1	14
115	Ag@Au Core–Shell Porous Nanocages with Outstanding SERS Activity for Highly Sensitive SERS Immunoassay. Sensors, 2019, 19, 1554.	2.1	12
116	Highly selective and efficient electroreduction of CO <sub>2</sub> in water by quaterpyridine derivativeâ€based molecular catalyst noncovalently tethered to carbon nanotubes. SmartMat, 2022, 3, 151-162.	6.4	12
117	Biomass-Derived Fe <sub>2</sub> N@NCNTs from Bioaccumulation as an Efficient Electrocatalyst for Oxygen Reduction and Zn–Air Battery. ACS Sustainable Chemistry and Engineering, 2022, 10, 9105-9112.	3.2	12
118	catena-Poly[[tetra-μ-acetatodinickel(II)]μ-N,N′-hexamethylenetetramine]. Acta Crystallographica Section E: Structure Reports Online, 2002, 58, m242-m244.	0.2	11
119	1,4-Diazoniabicyclo[2.2.2]octane hexaaquacobalt(II) bis(sulfate). Acta Crystallographica Section E: Structure Reports Online, 2005, 61, m671-m672.	0.2	11
120	Oxidative Coupling of Aromatic Amines and Nitrosoarenes: Iodineâ€Mediated Formation of Unsymmetrical Aromatic Azoxy Compounds. Advanced Synthesis and Catalysis, 2018, 360, 3150-3156.	2.1	11
121	Polymer–Inorganic Thermoelectric Nanomaterials: Electrical Properties, Interfacial Chemistry Engineering, and Devices. Frontiers in Chemistry, 2021, 9, 677821.	1.8	11
122	Bioinspired, Nanostructure-Amplified, Subcutaneous Light Harvesting to Power Implantable Biomedical Electronics. ACS Nano, 2021, 15, 12475-12482.	7.3	11
123	Controllable and Scale-Up Synthesis of Nickel-Cobalt Boride@Borate/RGO Nanoflakes via Reactive Impingement Mixing: A High-Performance Supercapacitor Electrode and Electrocatalyst. Frontiers in Chemistry, 2022, 10, 874675.	1.8	11
124	Crystallization regulation of solution-processed two-dimensional perovskite solar cells. Journal of Materials Chemistry A, 2022, 10, 13625-13650.	5.2	11
125	catena-Poly[[[aquazinc(II)]-μ-2,2′-dithiodibenzoato] bis(N,N-dimethylformamide)]. Acta Crystallographica Section E: Structure Reports Online, 2004, 60, m413-m415.	0.2	10
126	Self-assembled Three-dimensional Hierarchical BiVO4 Microspheres from Nanoplates: Malic Acid-assisted Hydrothermal Synthesis and Photocatalytic Activities. Chemistry Letters, 2009, 38, 962-963.	0.7	10

#	Article	IF	CITATIONS
127	An Ultra-low-cost Route to Mesostructured TS-1 Zeolite for Efficient Catalytic Conversion of Bulk Molecules. Industrial & Engineering Chemistry Research, 2014, 53, 13903-13909.	1.8	10
128	A Novel Design of High-Temperature Polymer Electrolyte Membrane Acetone Fuel Cell Sensor. Sensors and Actuators B: Chemical, 2021, 329, 129006.	4.0	10
129	A rapid green route for fabricating efficient SERS substrates. Green Chemistry, 2011, 13, 2831.	4.6	9
130	Intrinsic dew-enhancing ability of SiO2/PODS materials. Colloids and Surfaces A: Physicochemical and Engineering Aspects, 2011, 377, 110-114.	2.3	9
131	Cost-Effective Production of Pure Al13 from AlCl3 by Electrolysis. Industrial & Engineering Chemistry Research, 2012, 51, 11201-11206.	1.8	9
132	The selective formation of graphene ranging from two-dimensional sheets to three-dimensional mesoporous nanospheres. Nanoscale, 2014, 6, 7204-7208.	2.8	9
133	Gold Embedded Maghemite Hybrid Nanowires and Their Gas Sensing Properties. ACS Applied Materials & Interfaces, 2015, 7, 10534-10540.	4.0	9
134	Hybride organischâ€anorganische thermoelektrische Materialien und Baueinheiten. Angewandte Chemie, 2019, 131, 15348-15370.	1.6	9
135	Continuous impinging in a two-stage micromixer for the homogeneous growth of monodispersed ultrasmall Ni–Co oxides on graphene flakes with enhanced supercapacitive performance. Materials Chemistry Frontiers, 2021, 5, 4700-4711.	3.2	9
136	Kinetics and mechanism of the reaction between thiourea and iodate in unbuffered medium. Science in China Series B: Chemistry, 2004, 47, 480.	0.8	8
137	The propagation properties and kurtosis parametric characteristics of Hermite-cosh-Gaussian beams passing through fractional Fourier transformation systems. Optik, 2005, 116, 461-468.	1.4	8
138	Fabrication of Te@Au core-shell hybrids for efficient ethanol oxidation. Journal of Power Sources, 2012, 215, 227-232.	4.0	8
139	Fabrication of Te@Pd Core–Shell Hybrids for Efficient C–C Coupling Reactions. Journal of Physical Chemistry C, 2012, 116, 7416-7420.	1.5	8
140	Photoelectrochemical chiral sensing on the basis of TiO2–metal complex hybrid film. Journal of Electroanalytical Chemistry, 2012, 674, 97-102.	1.9	8
141	Titanium and nitrogen co-doped porous carbon for high-performance supercapacitors. Materials Chemistry Frontiers, 2021, 5, 3628-3635.	3.2	8
142	Thermal and FTIR spectral studies of N,N′-diphenylguanidine. Journal of Thermal Analysis and Calorimetry, 2012, 110, 593-599.	2.0	7
143	Synthesis of Î <sup>2</sup> -amino alcohols using the tandem reduction and ring-opening reaction of nitroarenes and epoxides. Tetrahedron, 2016, 72, 3839-3843.	1.0	7
144	The significance of different heating methods on the synthesis of CdS nanocrystals. RSC Advances, 2016, 6, 28229-28235.	1.7	7

#	Article	IF	CITATIONS
145	One-Pot Synthesis of α,β-Unsaturated Esters, Ketones, and Nitriles from Alcohols and Phosphonium Salts. Synthesis, 2018, 50, 107-118.	1.2	7
146	Highly Stable Low-Cost Electrochemical Gas Sensor with an Alcohol-Tolerant N,S-Codoped Non-Precious Metal Catalyst Air Cathode. ACS Sensors, 2021, 6, 752-763.	4.0	7
147	Hydroxylated Multiâ€Walled Carbon Nanotubes Covalently Modified with Tris(hydroxypropyl) Phosphine as a Functional Interlayer for Advanced Lithium–Sulfur Batteries. Angewandte Chemie, 2022, 134, .	1.6	7
148	Enhanced Selective Photooxidation of Toluene to Benzaldehyde over Co <sub>3</sub> O <sub>4</sub> â€Modified BiOBr/AgBr S‣cheme Heterojunction. Solar Rrl, 2022, 6, .	3.1	7
149	Photoelectrocatalytic oxidation of GMP on an ITO electrode modified with clay/[Ru(phen)2(dC18bpy)]2+ hybrid film. Science in China Series B: Chemistry, 2009, 52, 318-324.	0.8	6
150	Three silver(I) coordination polymers assembled from 2-sulfoterephthalic acid and N-donor ligands: syntheses, crystal structures, and luminescence properties. Transition Metal Chemistry, 2013, 38, 865-871.	0.7	6
151	Enhanced Interfacial Properties of Thickness-Tunable Carbon Nanosheets for Advanced Lithium–Sulfur Batteries. Energy & Fuels, 2021, 35, 13419-13425.	2.5	6
152	Synthesis, crystal structures and characterization of three cadmium(II) metal–organic coordination complexes constructed from flexible bis(imidazole) and carboxybenzaldehyde ligands. Journal of Molecular Structure, 2014, 1068, 149-154.	1.8	5
153	Facile synthesis of α, β-unsaturated esters through a one-pot copper-catalyzed aerobic oxidation-Wittig reaction. Tetrahedron Letters, 2018, 59, 14-17.	0.7	5
154	Oneâ€step facile synthesis of PbS quantum dots/Pb (DMDC) 2 hybrids and their application as a lowâ€cost SERS substrate. Journal of Raman Spectroscopy, 2019, 50, 1445-1451.	1.2	5
155	Synthesis of Unsymmetrical Aromatic Azoxy Compounds by Silverâ€Mediated Oxidative Coupling of Aromatic Amines with Nitrosoarenes. Advanced Synthesis and Catalysis, 2019, 361, 1394-1399.	2.1	5
156	Copper-Catalyzed Aerobic Oxidative Cyclization of 2-Alkynylanilines with Nitrosoarenes: Synthesis of Organic Solid Mechanoluminescence Compounds of 4-Oxo-4 <i>H</i> -cinnolin-2-ium-1-ide. Organic Letters, 2021, 23, 1228-1233.	2.4	5
157	Kinetics of the thermal decomposition of diethyldithiocarbamato tellurium (IV). Thermochimica Acta, 2006, 451, 94-98.	1.2	4
158	The Synthesis and Anticancer Activities of Peptide 5-fluorouracil Derivatives. Journal of Chemical Research, 2009, 2009, 261-264.	0.6	4
159	Growth of Singleâ€Walled Carbon Nanotubes from Tellurium Nanoparticles by Alcohol CVD. Chemical Vapor Deposition, 2010, 16, 136-142.	1.4	4
160	Van der Waals Templateâ€Assisted Lowâ€Temperature Epitaxial Growth of 2D Atomic Crystals. Advanced Functional Materials, 2022, 32, .	7.8	4
161	2,3,5,6-Tetramethylpyrazine–p-nitrophenol (1/2). Acta Crystallographica Section E: Structure Reports Online, 2005, 61, o614-o615.	0.2	3
162	Nonlinear Oxidation of Thiourea in an Unbuffered Medium. Chinese Journal of Chemistry, 2008, 26, 1771-1779.	2.6	3

#	Article	IF	CITATIONS
163	CVD growth of high density SWNTs network on surface using iron phosphide nanorods as catalyst precursor. Chemical Physics Letters, 2008, 464, 49-53.	1.2	3
164	Fabricating two-dimensional nanostructured tellurium thin films via pyrolyzing a single-source molecular precursor. Thin Solid Films, 2010, 518, 4215-4220.	0.8	3
165	Porous Carbon Spheres with Ultra-fine Fe2N Active Phase for Efficient Electrocatalytic Oxygen Reduction. Journal of Electronic Materials, 2021, 50, 3078-3083.	1.0	3
166	Advanced TexSy-C Nanocomposites for High-Performance Lithium Ion Batteries. Frontiers in Chemistry, 2021, 9, 687392.	1.8	3
167	μ1,3-Azido-diazidotetrakis(1,10-phenanthroline)dicopper(II) azide tetrahydrate. Acta Crystallographica Section C: Crystal Structure Communications, 2002, 58, m12-m13.	0.4	2
168	catena-Poly[[(1,10-phenanthroline-κ2 N,N′)copper(II)]-μ-(dihydrogen benzene-1,2,4,5-tetracarboxylato)-κ2 O 1:O 4]. Acta Crystallographica Section C: Crystal Structure Communications, 2003, 59, m454-m455.	0.4	2
169	catena-Poly[[aqua(nitrato-κ2O,O′)(1,10-phenanthroline)cadmium(II)]-μ-nitrato-κ2O:O′]. Acta Crystallographica Section E: Structure Reports Online, 2005, 61, m1058-m1060.	0.2	2
170	Electrochemical investigation on the interaction of benzene sulfonyl 5-fluorouracil derivatives with double-stranded DNA and G-quadruplex DNA. Science China Chemistry, 2012, 55, 1345-1350.	4.2	2
171	Fabrication of Noble-Metal Catalysts with a Desired Surface Wettability and Their Applications in Deciphering Multiphase Reactions. ACS Applied Materials & Interfaces, 2013, 5, 3952-3958.	4.0	2
172	Rücktitelbild: Polymerâ€Templated Formation of Polydopamineâ€Coated SnO <sub>2</sub> Nanocrystals: Anodes for Cyclable Lithiumâ€Ion Batteries (Angew. Chem. 7/2017). Angewandte Chemie, 2017, 129, 1958-1958.	1.6	2
173	Surface Wettability-Enhanced Electrochemical Detection of Hydrogen Peroxide. International Journal of Electrochemical Science, 2017, , 4479-4487.	0.5	2
174	Efficient Electrochemical Reduction of Oxygen Catalyzed by Porous Carbon Containing Trace Amount of Metal Residues. Electroanalysis, 2018, 30, 2768-2773.	1.5	2
175	Alkaliâ€Ion Batteries: SnO <sub>2</sub> as Advanced Anode of Alkaliâ€Ion Batteries: Inhibiting Sn Coarsening by Crafting Robust Physical Barriers, Void Boundaries, and Heterophase Interfaces for Superior Electrochemical Reaction Reversibility (Adv. Energy Mater. 6/2020). Advanced Energy Materials. 2020. 10. 2070027.	10.2	2
176	1,4-Diazoniabicyclo[2.2.2]octane diaquabis(pyrazole-3,5-dicarboxylato)zincate(II) dihydrate. Acta Crystallographica Section E: Structure Reports Online, 2005, 61, m702-m704.	0.2	1
177	Theoretical analysis on the structure and properties of thiourea dioxide crystal. Molecular Simulation, 2007, 33, 975-978.	0.9	1
178	One-step synthesis of metal sulfide/tellurium composites with distinct microstructures. Canadian Journal of Chemistry, 2015, 93, 1076-1082.	0.6	1
179	Controllable Synthesis of Fusiform-shaped Te@Au hybrids for Efficient Electrocatalytic Oxidation of Isopropanol. International Journal of Electrochemical Science, 2017, , 2441-2452.	0.5	1

 $R\tilde{A}^{1/4}$ cktitelbild: A Single $\hat{a} \in A$ tom Iridium Heterogeneous Catalyst in Oxygen Reduction Reaction (Angew.) Tj ETQq0 0.0 rgBT /Overlock 10 I.6 rgBT /Overlock 10 II.6 rgBT /O

#	Article	IF	CITATIONS
181	Carbon energy: A multidisciplinary exploration of energy technologies and carbon materials science. , 2019, 1, 4-5.		1
182	Perovskite Solar Cells: Synergistic Cascade Carrier Extraction via Dual Interfacial Positioning of Ambipolar Black Phosphorene for Highâ€Efficiency Perovskite Solar Cells (Adv. Mater. 28/2020). Advanced Materials, 2020, 32, 2070211.	11.1	1
183	Synthesis of Unsymmetrical Azoxyarenes via Copper atalyzed Aerobic Oxidative Dehydrogenative Coupling of Anilines with Nitrosoarenes. Advanced Synthesis and Catalysis, 2021, 363, 1963-1967.	2.1	1
184	Nonlinear Dynamics in KIO <sub>4</sub> -SC(NH <sub>2</sub> ) <sub>2</sub> -H <sub>2</sub> SO <sub>4</sub> Reaction System. Wuli Huaxue Xuebao/ Acta Physico - Chimica Sinica, 2002, 18, 264-267.	2.2	1
185	Tetramethylpyrazine–endo-norbornene-cis-5,6-dicarboxylic acid (1/2). Acta Crystallographica Section E: Structure Reports Online, 2005, 61, o731-o732.	0.2	0
186	6,6′-Dioxo-2,2-bi(7-oxatricyclo[3.2.1.13,8]nonane)-4,4′-dicarboxylic acid. Acta Crystallographica Section E: Structure Reports Online, 2005, 61, o1196-o1197.	0.2	0
187	Electrocatalytic oxidation of GMP on an ITO electrode modified by the photodeposition of Pd nanoparticles onto a monolayer TiO2 nanosheets/[Ru(phen)2(dC18bpy)]2+ hybrid film. Science China Chemistry, 2011, 54, 483-489.	4.2	0
188	[In(C2O4)(C7H3N1O4)2(H2O)4]·2H2O, C16H18In2N2O18. Zeitschrift Fur Kristallographie - New Crystal Structures, 2012, 227, 367-368.	0.1	0
189	One-pot synthesis of dumbbell shaped PbS–Te hybrids with promising photothermal properties. Canadian Journal of Chemistry, 2020, 98, 799-805.	0.6	0